



**HAL**  
open science

# Using Dynamic Time Warping for Ultrasonic Sheet Metal Welding monitoring

Elie Abi Raad, Michael Vorländer

► **To cite this version:**

Elie Abi Raad, Michael Vorländer. Using Dynamic Time Warping for Ultrasonic Sheet Metal Welding monitoring. Forum Acusticum, Dec 2020, Lyon, France. pp.2309-2315, 10.48465/fa.2020.0521 . hal-03240279

**HAL Id: hal-03240279**

**<https://hal.science/hal-03240279>**

Submitted on 29 May 2021

**HAL** is a multi-disciplinary open access archive for the deposit and dissemination of scientific research documents, whether they are published or not. The documents may come from teaching and research institutions in France or abroad, or from public or private research centers.

L'archive ouverte pluridisciplinaire **HAL**, est destinée au dépôt et à la diffusion de documents scientifiques de niveau recherche, publiés ou non, émanant des établissements d'enseignement et de recherche français ou étrangers, des laboratoires publics ou privés.

# Using Dynamic Time Warping for Ultrasonic Sheet Metal Welding Monitoring

Elie Abi Raad

Michael Vorländer

Institute for Technical Acoustics, RWTH Aachen, Germany  
ear@akustik.rwth-aachen.de

## ABSTRACT

Ultrasonic Metal Welding (USMW) is a friction welding process in which metal workpieces are welded together. The process is commonly used in the industry. However, even when given the same welding parameters, the strength of the weld can vary, and many factors can influence it. Currently, not enough is known about the welding process to be able to accurately control the quality of the weld during welding. Nevertheless, there is a consensus in the literature that the process happens in multiple stages. These stages are characterized by different bond strengths, such that different stages will have different distinctive vibrations of the welding tools at different frequencies. This paper uses Dynamic Time Warping (DTW) to analyze measurements of the vibrations of the sonotrode and anvil and of the sound emitted during welding when welding thin copper sheets with different welding times. By measuring the similarities between the signals, DTW helps identify the best combination of sensor and frequency band to monitor the welding process.

## 1. INTRODUCTION

Ultrasonic Metal Welding, also called USMW for short, is a friction-welding process. It is often used when precise welding of small components is required, or when dissimilar metals have to be welded, for example when manufacturing electronic components. USMW works by first placing two workpieces, which are the metal pieces that have to be welded, on top of each other on a flat surface, called “the anvil”. Then, a machine component called “sonotrode” compresses the workpieces against each other. Finally, the sonotrode vibrates horizontally, and induces a relative motion between the workpieces. This is when welding starts. The relative motion between the workpieces produces friction between them, which heats them up and increases their temperatures. The workpieces become more ductile. This leads to the formation of microwelds between the workpieces, what is described as stage 3 in [1]. As welding continues, the number of microwelds increases until an optimal number is reached (stage 4). If welding continues for too long, the microwelds start to break (stage 5). A summary of the welding stages as described in [1] is given in **Table 1**. More descriptions of USMW can be found in [2], [3], [4], [5] and [6].

To weld the workpieces together, the machine operator has to give the welding machine a variety of input parameters. These parameters depend on the material properties of the workpieces and their geometry. They include, among other parameters, the pressure to be applied on the workpieces and the total duration of

welding, which controls the amount of energy that goes into the system. The welding parameters are chosen based on the experience of the machine operator and trial and error. However, even when using the same welding parameters and for seemingly similar workpieces, it is common to have fluctuations in the strengths of the welds. There are many possible reasons for this. slight differences in the material properties of the workpieces, differences in alignment between different welds, or even heating of the machine due to repetitive welds. Since controlling all these parameters prior to each weld would greatly increase the preparation time for USMW and decrease its attractiveness, the alternative to produce the strongest welds is to use a real-time monitoring system that can monitor the welding process, recognize when the strongest weld is about to be obtained, and stop the welding process then. At this point in time, and to the knowledge of the authors, no such system is already implemented in the industry.

It might be possible to use the vibrations of the anvil and sonotrode during welding to monitor the welding process. Their vibrations depend on the strength of the bond between the workpieces. In UWMS, the source of vibrations is the sonotrode. Its vibrations are transmitted through the workpieces to the anvil. the stronger the connection between the workpieces, the stronger the connection between the sonotrode and anvil (assuming no slipping), the larger the vibrations in the anvil, and the smaller the vibrations in the sonotrode due to the extra loading from the anvil. As welding progresses, the weld becomes stronger through its stage 3 until it reaches a plateau in its stage 4, and then becomes weaker through its stage 5 [1][6]. Through this connection, the transfer of vibrations to the anvil and the loading on the sonotrode change during welding, and leading to changes in their vibrations.

Welding stages	Description
Stage 1	Compression of the workpieces. No vibrations.
Stage 2	Vibrations start, temperature increases, yield strength decreases. No weld yet.
Stage 3	Microwelds start to form. Strength of the bond increases.
Stage 4	Optimal number of microwelds. Strongest weld.
Stage 5	Fatigue of the microwelds, failure of some microwelds. Strength decreases.

**Table 1.** Welding happens in stages, and the bond strength of the weld changes in time and from stage to stage.

In [7], the authors presented a series of measurements of the vibrations of the sonotrode and anvil during welding, as well as the sound pressure emitted during welding. By stopping the welding process at roughly three different times, they produced three types of welds. Underwelds, which are the weaker welds welded until stage 3, Basic welds, which had the optimal welding time and were welded until stage 4, and Basic welds+, which are longer basic welds closer to over-welding, and are somewhere between stages 4 and 5. The welding times were chosen by trial and error to be approximately within these stages. Then, by filtering the measurements around the welding frequency (20 kHz) and its harmonics up to 80 kHz, the authors found that the vibrations of the sonotrode showed the most distinctive changes during welding, while the anvil vibrations were less distinctive, and the sound pressure measurements showed no distinctive patterns. The raw data in this work is the same as the one presented in [7].

Since the vibrations of the sonotrode showed distinctive changes when filtered at different frequencies, the next question is to know which frequency would be most appropriate to monitor the welding process. The best choice should show the most differences between the vibrations of stages 3 and 4, so that the beginning of stage 4 can be recognized, and between stages 4 and 5, to avoid going into overwelding. Due to the high numbers of signals, an automated comparison algorithm is preferred. In addition, as can be seen in **Figure 1**, even for welds done with the exact same time setting, the start time and end time are different. The duration of the signals can also be different, which would mean that the stage welding stage takes a different amount of time in different measurements. The algorithm should therefore be able to cope with the different start and end times, and should find the best fit between the signals so that welding stages on one signal are compared to the same welding stages of the other signal.

For those reasons, Dynamic Time Warping (DTW) was chosen. DTW is a similarity measurement algorithm that measures the similarity between two time signals. To do that, the algorithm finds the optimal alignment between the two signals by comparing all the samples of the signals to each other, testing all possible alignments, and choosing the one with the best fit. The signals can have different start times, end times, or lengths in time. DTW also aligns similar features of the signals, such as changes of direction in a curve, if they are shifted in time. This is useful to deal with the different durations of the different welding stages, which would shift important features away from each other, such as peaks or inflection points. A third feature of DTW is that it computes a score that describes how different the two time signals are from each other. This score is often called the distance, and is the sum of the differences between the two signals. If two signals are similar, the distance is smaller than if the signals are different. An example of DTW is shown in **Figure 1**. Two signals, envelopes of the sonotrode vibrations filtered around 20 kHz, have different start times, end times, and lengths in time. The DTW finds the best fit between them, aligns them, and outputs two

signals that are optimally matched to each other. It is worth noting that, due to its functioning, DTW is impervious to permutations of its input signals, such that comparing a signal A to another signal B returns the same result as comparing the second signal B to the first signal A [9][10][11].

The work in this paper analyzes the data from the sonotrode, anvil and microphone presented in [7] to find which combination of tool and frequency band would be most promising to monitor welding through its different stages. Using DTW to compare the signals from the same sensor and frequency band and from different welding stages, the best sensor and frequency combination or combinations will be chosen as the one with the most potential to easily and accurately monitor welding.

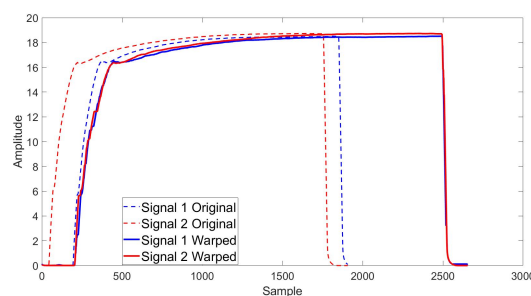


**Figure 1.** Example of DTW on the sonotrode vibrations at 20 kHz. The dashed red and blue lines are the original signals, and the full lines are the signals after warping by DTW. The output lines have the same start and end, and only differ by their amplitudes.

## 2. METHODOLOGY

To find the combination of sensor and frequency band best suited to monitor welding, DTW was used to compare measurements of the vibrations of the sonotrode, measurements of the vibrations of the anvil, and measurement of the sound pressure during welding. The experimental setup is detailed in [7], and the same raw data is used in this work. A review of the essentials is given here. In short, many workpieces, all copper sheets of dimensions 125 mm x 45 mm x 0.5 mm and with cleaned surfaces, were ultrasonically welded. The welding pressure was kept constant during welding, and the welding time was set to one of three different times, such that Underwelds, Basic welds and longer Basic welds, referred to as Basic welds +, could be produced. The result was 21 underwelds, 26 basic welds and 27 basic welds +. The velocities of the vibrations of the sonotrode and anvil were measured during welding using Laser Doppler Vibrometers, and then integrated to get the displacements, while the sound pressure was measured with an omnidirectional microphone placed 50 cm away from the welding site. The data was then filtered around the welding frequency (20 kHz) and its harmonics (40 kHz, 60 kHz, 80 kHz) in 1 kHz bands.

Afterwards, the filtered data was processed to prepare for DTW using the steps described in section 3.1 of this paper. Furthermore, as seen in **Figure 2**, **Figure 3** and **Figure 4**, the signals from the same welding type, sensor

and frequency band can be very similar or very different. For a reliable monitoring of welding, it is preferred to monitor a signal with low variance. Therefore, for each weld type, sensor and frequency band, reference envelopes were produced from all the envelopes in the respective categories by taking the median of each sample of the envelopes. This is described in more details in section 3.2 of this paper. These reference envelopes are then compared to all the envelopes from the same welding type to test the amount of spread of the signals at the respective sensor and frequency band. The reference envelopes are also compared to all the envelopes from the other welding types, keeping the frequency band and sensor constant. Envelopes that are similar to the reference envelope return lower distance scores than envelopes that are more different. Finally, looking at the distribution of scores, the sensor and frequency band with the biggest differences in the DTW scores is chosen as the most promising frequency for monitoring. Two cases are possible when comparing the scores. If the scores of the reference signal of welding type underwelds (U) compared to the same weld type U are similar to the scores of U compared to the welding type basic welds (B), then it is unclear whether the signals are different. On the contrary, if the scores are noticeably lower for U compared to U, then the signals of U are noticeably different from those of B. In that case, the sensors at that specific sensor and frequency band could be used to monitor the change from U to B.

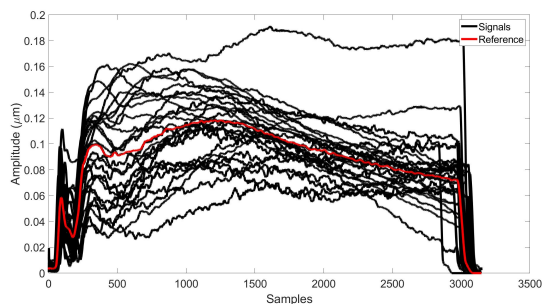


**Figure 2.** Envelopes (black) and reference (red) of anvil vibrations at 40 kHz

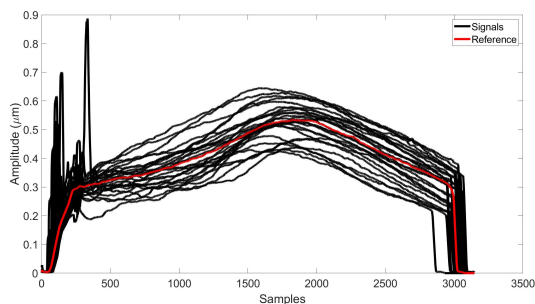


**Figure 3.** Envelopes (black) and reference (red) of sonotrode vibrations at 40 kHz

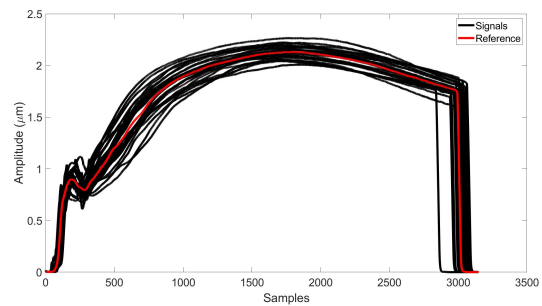


**Figure 4.** Envelopes (black) and reference (red) of sonotrode vibrations at 60 kHz

### 3. PROCESSING THE DATA

#### 3.1 Processing for DTW

The raw data was processed so that DTW could be applied to the envelope of the signals filtered in frequency bands. First, the raw data was filtered in 1 kHz bands around the welding frequency, 20 kHz, and its harmonics, 40 kHz, 60 kHz and 80 kHz. Then, from the filtered signals, the positive envelope of the data of each weld was taken, smoothed using a moving average of window size 0.01 s (about 1% of the welding time), and downsampled by a factor of 100 to speed up the run time of the algorithm. Compared to taking the full envelope, taking the positive envelope was enough. Due to the nature for the signal, the vibrations are symmetric oscillations around a rest position, and if positive displacement values mean the surface is moving away, then negative displacement values mean the surface is moving closer by a similar amount. Therefore, the negative envelope, as processed previously, would contain the exact same information as the positive envelope, with no additional information. A sample signal after these steps is shown in **Figure 5**.

Then, to remove unnecessary sources of error in the algorithm, the start and end of the signals were truncated, after which each signal was normalized by dividing by its maximum. Normalizing the data was necessary because different signals, which were otherwise very similar and displayed the same trend, sometimes had different amplitudes. This difference in amplitude might be due to the slight changes in measurement position of a vibrometer between welds, as it was adjusted for a better measurement. Since DTW only aligns the different signals in time and does not change their amplitude, the difference in amplitude would add a lot of superfluous error in the code, so the data was normalized. As for the start of the welds, it often contained high-amplitude peaks due to particles ejected during welding which interfered with the measurement. These peaks, when larger than the maximum of the signal, sometimes greatly affected its normalization. Examples of such peaks can be seen around sample 400 in **Figure 3**. The start was truncated before the start of stage 3, so as not to lose any important information. As for the end of the signal, it described the stop of welding, in which the sonotrode stopped its vibrations, and therefore did not describe the welding process. Keeping it would force the DTW to

align the ends of signals from different welding types to the same end, which caused problems when comparing signals from different weld types, so the ends were removed from the signals. **Figure 5** shows, in red, the approximate truncation lines for the sonotrode measurement at 20 kHz.

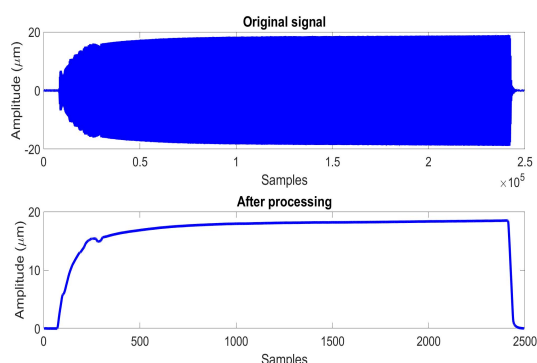


**Figure 5.** Top. raw signal from the sonotrode measurement at 20 kHz. Bottom. positive envelope after smoothing and downsampling. In red. the truncation limits of the start and end.

### 3.2 Creating the reference welds

The signals were compared to reference welds produced by taking the median of all signals of a specific frequency, sensor, and weld type. for each sample  $n$ , the median of the  $n^{\text{th}}$  samples of all the signals of that weld type, sensor and frequency band was taken. For example, the median of the sonotrode underwelds at 40 kHz was produced sample by sample, by taking the median of the respective samples of all sonotrode underweld 40 kHz signals. The median was used instead of the mean because it is more robust against outliers, and would better deal with random peaks occurring in the signals. Examples of the reference signals and the envelopes they were produced from can be seen in **Figure 2**, **Figure 3** and **Figure 4**, with the reference in red, and the signals they are made from in black. The reference can sometimes fit the original data perfectly, as in **Figure 4**, or not so well, as in **Figure 2**.

## 4. RESULTS

In the following figures and text, a shorter notation system is used. underwelds are denoted by U, basic welds by B, and basic welds+ by O, as they are close to overwelds. Comparing the reference of the underwelds to other underwelds is then denoted by UU, and comparing it to basic welds is denoted by UB. the first letter denotes the type of the reference signal, and the second letter denotes the type of the other signals. Sample plots of the output of DTW are shown in Figures 6 to **Figure 12**. **Figure 6** to **Figure 10** show the effect of DTW for sonotrode vibrations at 60 kHz, which were found to be promising in [7]. **Figure 11** and **Figure 12** show the effect of DTW for anvil vibrations at 80 kHz. The thin lines are the original signals, scaled down by 1.25 so as to stay visible and not overlap with the warped signals, and the thick lines are the output of DTW, the warped signals.

**Figure 6** and **Figure 8** show UU and BB. As seen in the figures, the DTW algorithm has aligned the output, and there is a perfect match between the warped signals. As for UB and BO, shown in **Figure 7** and **Figure 9**, the misalignment is clear at the end of the signals. This is also apparent in the scores. UU and BB have scores of less than 1, while UB and BO have scores at least ten times larger. **Figure 10** also shows an example of DTW fitting two signals of the same welding type, OO, in which the start and end times are different, and in which the welding stages take different amounts of time. The median, in thin blue, starts increasing before the red signal, but reaches its peak later, indicating a longer stage 3 for the median. The median also ends later than the signal, so the lengths of the respective stage 4 are also different. DTW was able to find an almost perfect fit between the two signals, aligned their inflection points, and outputted a score that was lower than BO.

**Figure 11** and **Figure 12** show the output of DTW aligning the same reference signal to signals from two different welding types, BB and BO. In this case, DTW aligned the envelopes of the different groups better than the envelopes from the same group. Contrary to the sonotrode example at 60 kHz, here, DTW found that the B and O signals were more similar than the B and B signals, scoring about 15 for the former and 8 for the latter. In the right part of Figure 10, one can even see where the B reference and the B signal diverge.

The results of the DTW algorithm are shown in **Figure 13** to **Figure 18**.

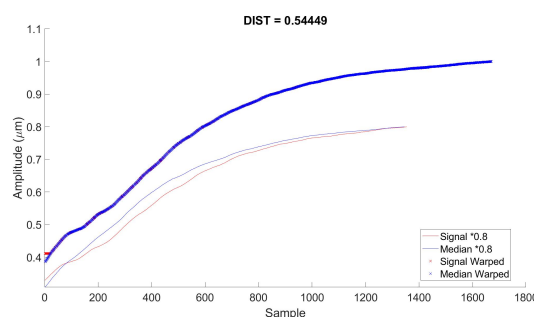


**Figure 6.** Sonotrode at 60 kHz. U vs U.

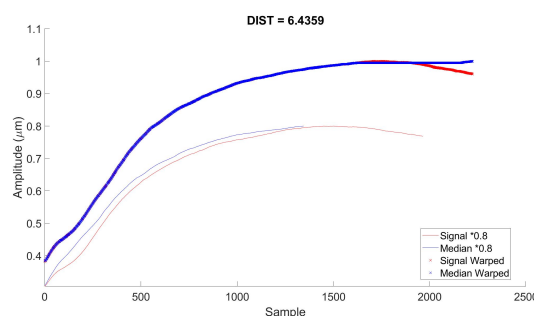


**Figure 7.** Sonotrode at 60 kHz. U vs B

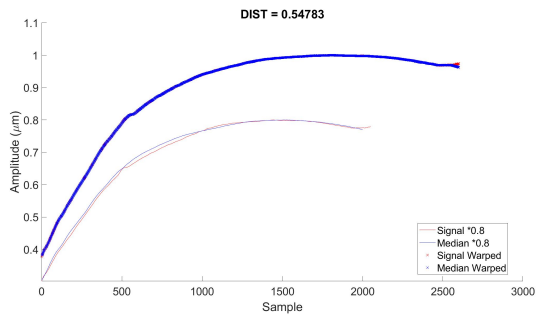


Figure 8. Sonotrode at 60 kHz. B vs B

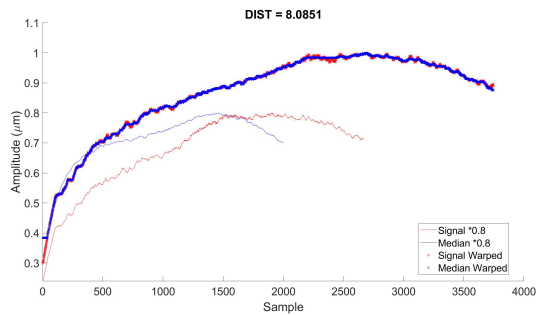


Figure 12. Anvil at 80 kHz. B vs O

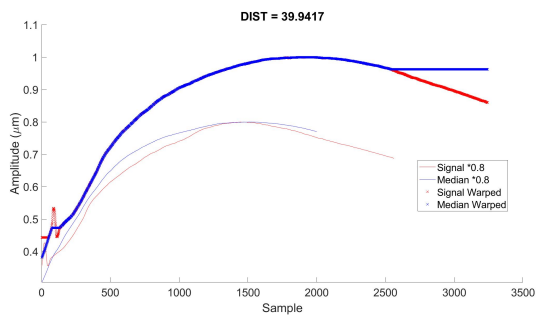


Figure 9. Sonotrode at 60 kHz. B vs O

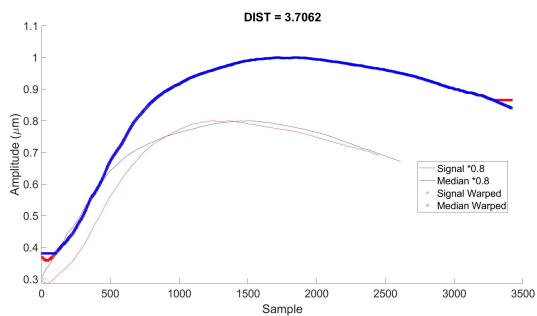


Figure 10. Sonotrode at 60 kHz. O vs O

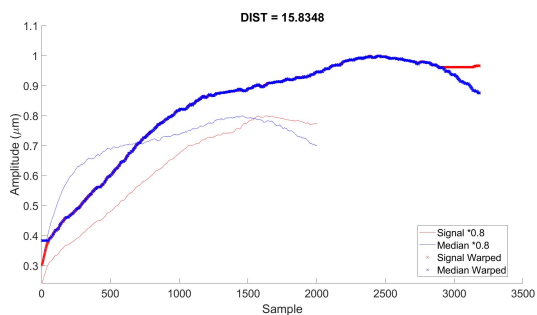


Figure 11. Anvil at 80 kHz. B vs B

#### 4.1 Sonotrode results

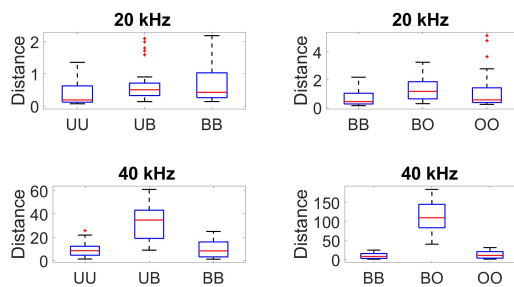


Figure 13. Distribution of the results for the sonotrode at 20 and 40 kHz.

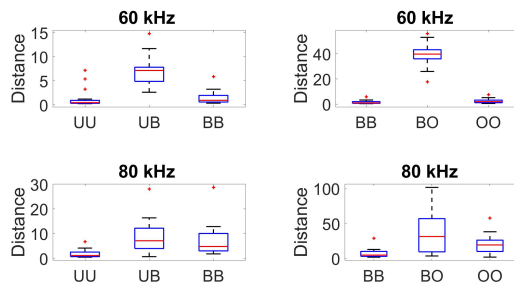


Figure 14. Distribution of the results for the sonotrode at 60 and 80 kHz.

#### 4.2 Anvil results

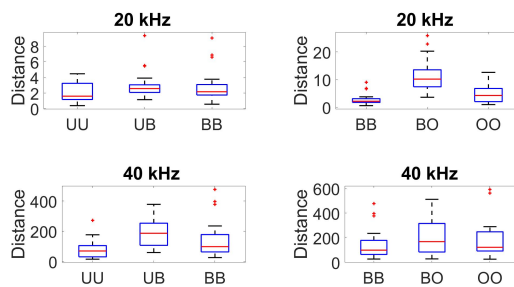
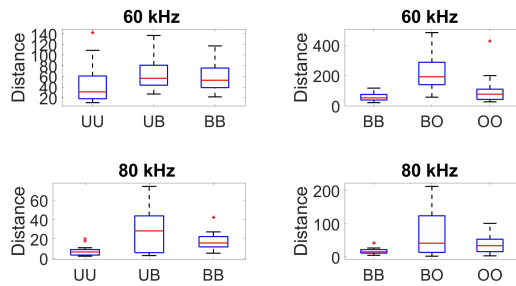
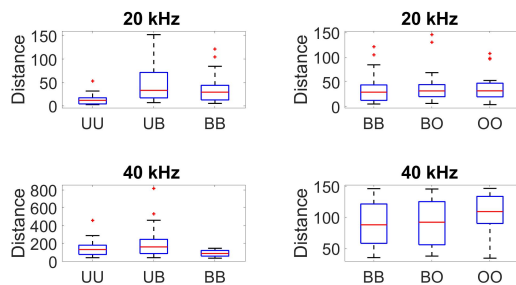


Figure 15. Distribution of the results for the anvil at 20 and 40 kHz.



**Figure 16.** Distribution of the results for the anvil at 60 and 80 kHz.

### 4.3 Microphone results



**Figure 17.** Distribution of the results for the microphone at 20 and 40 kHz.

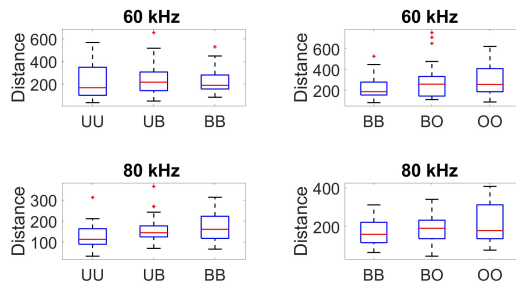


**Figure 18.** Distribution of the results for the microphone at 60 and 80 kHz.

## 5. ANALYSIS

DTW was able to successfully align signals with different start times, end times, and more importantly, different stage times and inflection points, as seen in **Figure 10**. Since different stage times show different vibration patterns, and inflection points might indicate important changes in the welding process, it is important that they do not get distorted in the similarity measurement. As such, DTW achieves what simple time shifting cannot. In addition, as seen in **Figure 11** and **Figure 12**, the scores DTW outputs do not depend on the signal length, and only on the similarity between the signals it compares.

Looking at the sonotrode results at 20 kHz and 80 kHz, one can see a lot of overlap in the boxplots for UU, UB, BB, BO and OO. This indicates no major difference between the signals at these frequencies. At 40 kHz and 60 kHz, the score distributions for BO are noticeably smaller than for BB and OO, with no overlap of boxplots.

The fact that BB and OO are relatively small indicates that the signals in B and O are similar to their respective reference signals, and that the larger scores in BO are due to differences between B and O, and not to any variations within these groups. At 40 kHz, there is some overlap between UU, UB and BO, while at 60 kHz, there is almost no overlap between them. Therefore, 60 kHz offers the clearest changes going from stage 3 to stage 4, and then stage 5. This result is partly similar to the conclusion in [7]. 60 kHz is still the most promising frequency band, but [7] saw the 20 kHz and 80 kHz frequency bands as potentially good bands, which is not the case here.

Looking at the anvil distributions at 40 and 80 kHz, there is a lot of overlap between the boxplots for UU, UB, BB, BO and OO, indicating that DTW saw no major difference between the U, B and O signals at these frequencies. The same is true at 20 kHz and 60 kHz for UU, BU and BB. At those frequencies, the only clear difference is between BB and BO, and the difference is more pronounced at 20 kHz. However, the boxplots for BO and OO overlap, indicating that the signals in O might not resemble their reference, and that part of the reason why BO is larger than BB is not only because vibrations in B and O are different, but also because the vibrations within each of these groups are different from each other. Therefore, only the anvil B reference at 20 kHz could be used to monitor the transition from basic welds to basic welds +, and avoid overwelds. It is interesting to note that, contrary to the conclusion of [7], the 80 kHz band was not chosen here as a potentially acceptable frequency band.

As for the sound pressure distributions, there is no clear difference for all the frequencies. The microphone recordings as measured in [7] cannot be used to monitor welding. This is similar to the results in [7].

Overall, the best results are given by the sonotrode measurements at 60 kHz. However, due to the difficulties in measuring the vibrations of the sonotrode, explained in [7], using the anvil for reference at 20 kHz should still be considered. This is an improvement from the conclusion in [7], which suggested two frequency bands for the sonotrode vibrations and two frequency bands for the anvil vibrations.

## 6. CONCLUSION

This paper presented a study into the use of Dynamic Time Warping (DTW) in monitoring Ultrasonic Sheet Metal Welding, using data gathered experimentally on one welding machine, and for one set of dimensions of copper sheets. The welds were of three types: underwelds, basic welds, and longer basic welds. The data included the vibrations of the sonotrode and anvil during welding, as well as the airborne sound emitted during the process. The processing of the data before DTW included filtering the data in 1 kHz bands around the welding frequency and its harmonics, taking the positive envelopes, smoothing them, downsampling them, truncating the start and end of the signals, and finally normalizing them to their respective maximums. In addition, reference signals were made from the original

signals by taking the median of each sample. Then, for each sensor and frequency band combination, DTW was used to compare the reference signals of each welding type to all the envelopes of that type and of the subsequent type. Looking at the distribution of scores, the optimal signals for monitoring welding were found to be the sonotrode signals at 60 kHz, which could potentially monitor both the passage from underwelding to basic welding and from basic welding to overwelding. If the sonotrode vibrations cannot be measured during welding, then the anvil vibrations at 20 kHz could be used to monitor basic welding and avoid overwelding. However, it might not detect the onset of basic welding clearly. As for DTW, it was found that, with the correct preprocessing of the data, it successfully warped signals of different start times, end times, total lengths, or duration of welding stages, to find the optimal fit between the signals, all the while conserving their important features, such as inflection points or the shapes of the curves. DTW also produced similarity scores that are not affected by the lengths of the signals, and reflect accurately the level of similarity between them. Effectively, by measuring the similarity between signals from different welding stages and finding the frequency band that offered the most changes across welding, DTW helped choose one of multiple sensor-frequency combinations for monitoring Ultrasonic Metal Welding.

## 7. ACKNOWLEDGEMENT

The authors would like to thank the German Research Foundation DFG for the support of the research work under grant number RE2755/52-1. The authors would also like to thank Paul Khoury Helou for their help in investigating similarity measurement algorithms as part of their internship.

## 8. REFERENCES

- [1] E. Abi Raad, I. Balz, U. Reisgen, M. Vorländer. "Investigation of the applicability of acoustic emission and vibration analysis to describe the thermo-mechanical mechanism during ultrasonic metal welding", *Proceedings of the 23rd International Congress on Acoustics*, pp. 4700-4707, 2019.
- [2] Y Y Zhao, D Li & Y S Zhang. "Effect of welding energy on interface zone of Al-Cu ultrasonic welded joint", *Science and Technology of Welding and Joining*, Vol.18, No.4, pp. 354-360, 2013.
- [3] J. Wodara, H. Herhold, "Ultraschallfügen und -trennen. Band 1 der Grundlagen der Fügetechnik". *DVS Verlag (Fachbuchreihe Schweißtechnik 151)*, Düsseldorf, Germany 2004.
- [4] J. Harthoorn. "Ultrasonic metal welding", *Dissertation*, Eindhoven, Netherlands 1978.
- [5] HT. Fujiia, Y. Goto, YS. Sato, H. Kokawa. "Microstructural evolution in dissimilar joint of Al alloy and Cu during ultrasonic welding," *Materials Science Forum*, pp. 2747-2752, 2014.

- [6] I.Balz, E. Abi Raad, E.Rosenthal, R.Lohoff, A.Schiebahn, U.Reisgen, M.Vorländer. "Process monitoring of ultrasonic metal welding of battery tabs using external sensor data", *Journal of Advanced Joining Processes*, Vol. 1, 2020
- [7] E. Abi Raad, I. Balz, U. Reisgen, M. Vorländer. "Derivation of characteristic vibroacoustic parameters in Ultrasonic Sheet Metal Welding", *Proceedings of the Deutsche Jahrestagung für Akustik*, pp. 1129-1132, 2020.
- [8] Lu Y, Song H, Taber GA, Foster DR, Daehn GS, Zhang W. "In-situ measurement of relative motion during ultrasonic spot welding of aluminum alloy using Photonic Doppler Velocimetry", *Journal of Materials Processing Technology*, pp. 431-440, 2016.
- [9] Yang Zhang and T. F. Edgar, "A robust Dynamic Time Warping algorithm for batch trajectory synchronization," *2008 American Control Conference*, pp. 2864-2869, 2008.
- [10] Keogh and M. Pazzani. "Derivative Dynamic Time Warping," *Proceedings of the 2001 SIAM International Conference on Data Mining*, pp. 1-11, 2001.
- [11] Zhao, L. Itti. "shapeDTW. shape Dynamic Time Warping", *Pattern Recognition*, Vol. 74, pp. 171-184, 2018.